Microchemical Journal 160 (2021) 105713

Contents lists available at ScienceDirect

Microchemical Journal

journal homepage: www.elsevier.com/locate/microc

Electrochemical impedimetric detection of kanamycin using molecular imprinting for food safety

Deniz Işık [a], Samet Şahin [b,*], Mustafa Oguzhan Caglayan [b], Zafer Üstündağ [a,*]

[a] Kütahya Dumlupınar University, Department of Chemistry, 43100 Kütahya, Turkey
[b] Bilecik Şeyh Edebali University, Department of Bioengineering, 11230 Bilecik, Turkey

ARTICLE INFO

Keywords:
Kanamycin
Sensor
Impedimetric analysis
Electrochemistry
Molecular imprinting

ABSTRACT

In this work, molecularly imprinted kanamycin (KAN) electrodes were prepared using electrochemical polymerization of pyrrole (Py). First, a glassy carbon electrode was coated with an optimized volume of graphene oxide (GC/GO) to provide a high surface area electrode. Py is then polymerized on GC/GO electrode using cyclic voltammetry in the presence of KAN following by KAN removal using HCl (GC/GO-pPy-KAN*). Electrode preparation steps were also optimized using microscopic, spectroscopic, and electrochemical methods. Finally, the analytical performance of the prepared GC/GO-pPy-KAN* electrode was investigated for the determination of KAN. The limit of detection and the detection range was calculated as 5 nM and 5 nM–1 μM, respectively. The precision, accuracy, and interference studies showed good precision and relative error with minimum interference for the chosen substances. Moreover, real sample analysis was also performed using 4 different milk samples with good recovery values. Consequently, a novel, simple, and sensitive sensor was developed using an easy and low-cost fabrication method for the detection of KAN in food samples such as milk.

1. Introduction

Kanamycin (KAN, (2R,3S,4S,5R,6R)-2-(aminomethyl)-6-[(1R,2R,3S,4R,6S)-4,6-diamino-3-[(2S,3R,4S,5S,6R)-4-amino-3,5-dihydroxy-6-(hydroxymethyl)oxan-2-yl]oxy-2 hydroxycyclohexyl] oxyoxane-3,4,5-triol) is an aminoglycoside antibiotic, which is fabricated by the fermentation of *Streptomyces kanamyceticus* [1] and widely used in the treatment of farm animal infections [2] caused by Gram-negative and Gram-positive bacteria [3]. However, the random use of KAN may increase bacterial resistance and cause accumulation of KAN residue, which threatens human health [2].

The overuse of KAN can cause adverse effects with ototoxicity [4], nephrotoxicity [5], neuromuscular locking effects [6], and allergic reactions [7]. The feedstocks from treated animals with veterinary drugs or animals exposed to biocidal poses a threat to anyone who consumes them. Therefore, many regulations have been put into motion for the maximum residue limits (MRLs) of residual KAN in food samples of such conditions [8].

Several analytical methods have been developed for the determination of KAN from food samples such as high-performance liquid chromatography, gas chromatography, and mass spectrometry still being the gold standards [9,10]. Moreover, simple and fast detection of KAN has also been reported in the literature using colorimetric [11], fluorometric [8,12], enzyme-linked immunosorbent analysis [13], surface plasmon resonance (SPR) [5], and electrochemical-based [14,15] detection strategies. However, the ease and cost aspects of such applications should be further improved.

Recently, molecular imprinting technology has become very popular among researchers working on sensor design [16]. Molecular prints of a molecule can be imprinted using a suitable polymer matrix and the resulting system is often called "molecularly imprinted polymer, (MIP)" [17]. There are different ways one can imprint a molecule on a polymer matrix such as covalent or non-covalent imprinting [18]. Non-covalent imprinting has some advantages over covalent imprinting because the target molecule won't form covalently-linked complexes with the polymer, hence more efficient imprinting is achieved [19]. Moreover, non-covalently imprinted molecules can be detached from the polymer matrix and reattach again which creates high-affinity binding sites for target molecules [18,20].

Imprinting of polymers using electrochemistry is one of the most common methods for MIP applications over chemical polymerization [21]. It is because both electrochemical methods and the MIP-based

* Corresponding authors.
E-mail addresses: samet.sahin@bilecik.edu.tr (S. Şahin), zustundag@gmail.com (Z. Üstündağ).

https://doi.org/10.1016/j.microc.2020.105713
Received 6 August 2020; Received in revised form 19 October 2020; Accepted 3 November 2020
Available online 7 November 2020

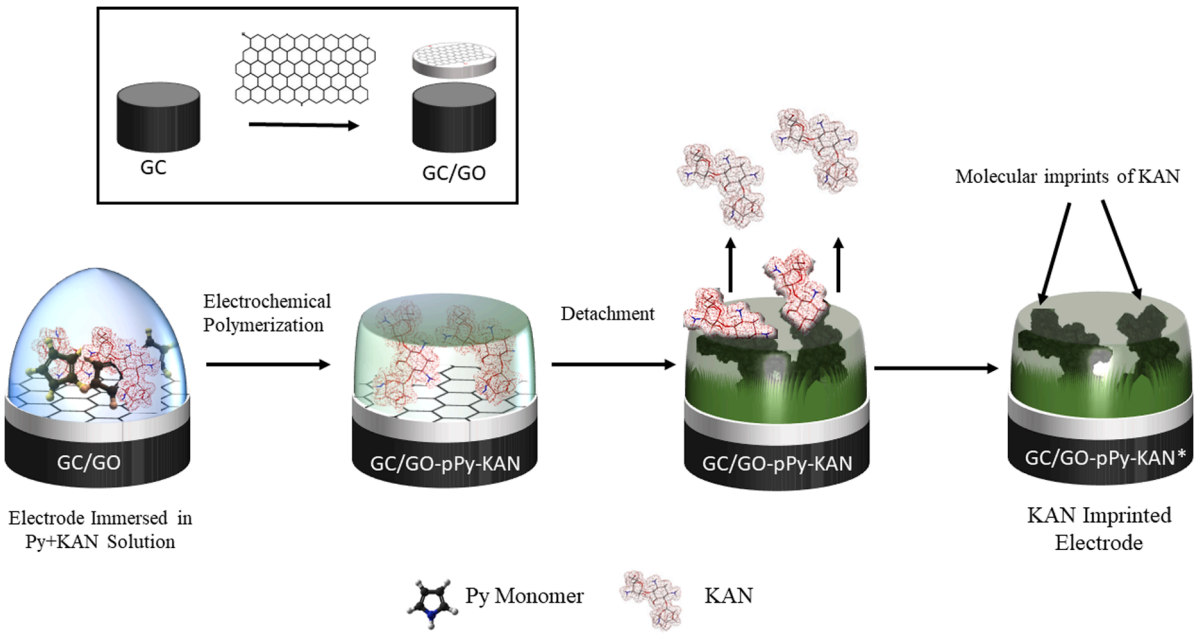

Fig. 1. Schematic representation of the steps of GC/GO-pPy-KAN* electrode preparation.

technologies are often low cost, highly stable, and sensitive, furthermore, they are suitable for integration with the current-state-of art technologies in the market [22]. Different types of polymers can be used for electrochemical polymerization such as poly(p-aminobenzene sulfonic acid)/o-phenylenediamine [23], methacrylic acid/ethylene glycol dimethacrylate [24] or polypyrrole (pPy) [25] among which pPy stands out due to its simple application. Graphene oxide (GO) and its derivates are one of the most exclusively studied nanomaterials due to its very high surface area and good electrical properties [26]. Once modified with GO, the surface area of the electrodes increases substantially providing a wide range and sensitive detection of target molecules especially for electrochemical-based sensing strategies [27–29].

In this work, a sensitive, MIP-based impedimetric KAN sensor was developed using electrochemical polymerization of Py as an imprinting template on GO modified glassy carbon (GC) electrode. All the steps of material synthesis and sensor fabrication steps were characterized using Raman, XPS, SEM, and electrochemical techniques (cyclic voltammetry (CV) and electrochemical impedance spectroscopy (EIS)). The optimization of different parameters for the fabrication of the MIP-KAN sensor and the analytical performance of the final sensor confirmation including real sample analysis was carried out using the EIS technique. In terms of methodology, this work offers an easy, low-cost, sensitive, and highly accurate way of determination of KAN from real samples such as milk.

2. Experimental

2.1. Materials

All chemicals used in this study were in HPLC grade and obtained from Merck, Fluka, Sigma-Aldrich, and Riedel. Kanamycin sulfate was obtained from Sigma-Aldrich. All aqueous solution and washing steps were performed using ultra-pure water (UPW, 18.2 MΩ cm) which was obtained from Human Power I (Human Corp., Korea). All electrochemical experiments were performed using a three-electrode system under high-purity argon (99.999%) atmosphere at room temperature (24 ± 1 °C) unless otherwise stated. The working electrode, counter electrode, and reference electrode were GC, Pt wire, and Ag/AgCl (Sat.) for the electrochemical tests, respectively. GCE was first polished with 100 and 50 μm alumina suspensions, washed with a mixture of acetonitrile-isopropyl alcohol (1:1, v:v), respectively, and sonicated with UPW in an ultrasonic bath for 5 min (Bandelin, Sonorex, 35 kHz) before use [30].

2.2. Synthesis of GO from graphite

GO is synthesized according to modified Hummer's method reported elsewhere [31]. Briefly, 2.5 g of graphite and 15 mL of H_2SO_4 were first well-mixed and 2.5 g of $K_2S_2O_3$ and 2.5 g P_2O_5 were added carefully. The mixture was then heated in the condenser for 6 h at 80 °C, filtered, and washed with UPW. The final product was placed in 125 mL of H_2SO_4 in a cooling bath. 15 g of $KMnO_4$ was slowly added by keeping the temperature below 20 °C. After the mixing, 250 mL of UPW was added and magnetically stirred for 4 h at 35 °C. After the final addition of 750 mL of UPW for dilution, 20 mL of 30% H_2O_2 was rapidly added and thoroughly mixed. The solution was stirred overnight and centrifuged at 10,000 rpm for 10 min. The precipitate was finally washed with 0.1 M HCl 3 times and GO is obtained after drying at 55 °C in a vacuum oven for 12 h [32].

2.3. Preparation of KAN imprinted electrodes

The schematic representation of the steps of KAN imprinted electrode preparation is shown in Fig. 1. First of all, 100 mg of the synthesized GO was dissolved in 5 mL of acetonitrile to obtain a suspension. Different volumes of the GO suspension were coated on freshly polished GC and dried under IR lamp (75 W) for 10 min (denoted as GC/GO).

Then, GC/GO electrode was immersed in 50 mM Py in phosphate buffer solution (PBS, in 0.1 M KCl, pH = 7) containing 5 different KAN concentrations; 10 mM, 15 mM, 20 mM, 25 mM, and 30 mM. Electrochemical polymerization was performed in a three-electrode set-up where GC/GO is the working electrode with 5 scans of CV at 50 mV/s scan rate between 0 and 1.8 V potential range. The optimum KAN concentration was determined using the EIS technique based on the charge transfer resistance (R_{ct}) changes and the polypyrrole (pPy)-KAN containing electrode were denoted as GC/GO-pPy-KAN.

Finally, KAN molecules were detached from GC/GO-pPy-KAN to obtain KAN imprinted electrode using a 0.01 M HCl solution (pH 2). The electrode was immersed in HCl solution and kept for 1, 5, 10, and 15 min under constant stirring, and the optimum time for the detachment procedure was determined. The KAN imprinted electrode was denoted

as GC/GO-pPy-KAN*.

2.4. Characterization of the materials and electrodes

The successful synthesis of GO was confirmed using Raman (Horiba, Jobin-Ivon, France) and SEM (Nova, NanoSEM-650, Belgium) techniques (Fig. S1). The formation steps of GC/GO-pPy-KAN* electrode surface were characterized using AFM (Park Systems AFM, NX10, S. Korea) and XPS (PHI 5000 VersaProbe, Japan/US) techniques. Finally, electrochemical characterization of all the electrode preparation steps and optimization studies were performed using CV and EIS techniques with an electrochemical analyzer (Ivium CompactStat, Netherlands). 1 mM of $K_3Fe(CN)_6/K_3Fe(CN)_6$ mixture was used as a redox probe for electrochemical analysis and all experiments were repeated 5 times unless otherwise stated (n = 5).

2.5. Development of KAN detection strategy using GC/GO-pPy-KAN* electrodes

In this work, KAN detection is performed using impedimetric analysis. The optimum conditions for GO coating on GC, KAN concentration for electropolymerization with Py, and the time needed for the detachment of KAN molecules were determined as described above. Lastly, the optimum time for KAN detection was determined using a 1 μM KAN standard sample for 10, 20, 30, and 40 min. GC/GO-pPy-KAN* electrode was dipped into 1 μM of KAN standard for a given time and optimum time required were determined using R_{ct} values obtained from EIS. The calibration range was selected between 5 nM and 1 μM KAN concentration. Nyquist plots were fitted based on the diffusion-controlled constant phase element equivalent circuit. Equivalent circuit models were also given in Table S1 [33].

Precision (relative standard deviation, RSD %) and accuracy measurements were conducted as intra-day and inter-day precision for 5 independent samples. Inter-day precision measurements were performed for 5 consecutive days. Non-specific interactions were also investigated using 1 μM tobramycin (TOB, (2S,3R,4S,5S,6R)-4-amino-2-{[(1S,2S,3R,4S,6R)-4,6-diamino-3-{[(2R,3R,5S,6R)-3-amino-6-(aminomethyl)-5-hydroxyoxan-2-yl]oxy}-2-hydroxycyclohexyl]oxy}-6-(hydroxymethyl)oxane-3,5-diol) and 1 μM gentamycin (GEN, (3R,4R,5R)-2-{[(1S,2S,3R,4S,6R)-4,6-diamino-3-{[(2R,3R,6S)- 3-amino-6-[(1R)- 1-(methylamino)ethyl]oxan-2-yl]oxy}-2-hydroxycyclohexyl]oxy}-5-methyl-4-(methylamino)oxane-3,5-diol) and 1 μM penicillin (PEN, 3,3-dimethyl-7-oxo-6-[(2-phenylacetyl)amino]-4-thia-1-azabicyclo[3.2.0]heptane-2-carboxylic acid), and 1 μM amoxicillin (AMX, (2S,5R,6R)-6-[[(2R)-2-amino-2-(4-hydroxyphenyl)acetyl]amino]-3,3-dimethyl-7-oxo-4-thia-1-azabicyclo[3.2.0]heptane-2-carboxylic acid). Interfering substances were tested in the presence of 10 nM KAN.

2.6. Real sample preparation for analysis

Commercial milk samples (4 samples) were purchased from a local supermarket and a pre-treatment was applied before analysis. 10 mL of each milk sample was first mixed with 1 mL of 10% trichloroacetic acid (% m/v) rapidly for about 30 s and immediately centrifuged at 5,000 rpm. The supernatant was removed and the precipitate was then washed with UPW following by second centrifugation. The supernatant was mixed with the latter and diluted with PBS for the analysis [34].

3. Results and discussion

3.1. Preparation and characterization of GC/GO-pPy-KAN* electrode

In this work, Py was chosen among different polymers that can be used for MIP. Py is preferred due to its biocompatible nature, electrical conductivity, and stability [35,36]. Furthermore, in situ electropolymerization of Py in the presence of a target molecule provides the fast and easy formation of MIP structure [37]. Therefore, pPy films on GC/GO electrode were obtained with the electropolymerization of Py in a PBS solution containing Py and KAN. Fig. 2 shows cyclic voltammograms for the electropolymerization of Py in PBS solution containing 50 mM Py and 25 mM KAN for five consecutive cycles in a scanning potential range from 0 V to +1.8 V (scan rate: 50 mV/s, pH 7). An oxidation peak at 0.7 V (vs Ag/AgCl) was first observed followed by a significant decrease in the peak current for the second cycle and reaching a stabilization current in the fifth cycle. The reason of the decreased peak current after the first scan could be related to the continuous formation of the pPy films obstructing the monomer access to the surface of the electrode [38]. This behavior is similar to that reported for the electropolymerization of Py with different molecules [25]. Furthermore, the mechanism of the electrochemical polymerization of pyrrole is an accepted phenomenon that is reported elsewhere [39].

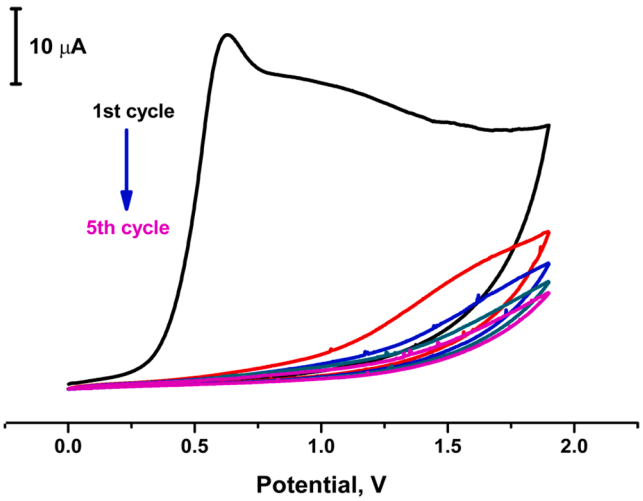

Fig. 2. CVs (scan rate 50 mV/s) for the electropolymerization of 50 mM Py on GC/GO electrode in PBS solution (pH 7) containing 25 mM KAN.

The peak current decrease with an increasing number of cycles indicates that the formation of pPy films with KAN molecules embedded in the polymer matrix hinders the electron transfer of the Py monomer [38]. The effect of the number of cycles applied certainly affects the morphology of the electrodes, such as thickness, due to the changing number of embedded KAN molecules in pPy film after each cycle. Therefore, the number of cycles applied was optimized to be five to keep the thickness of the film the same and obtain a more stable GC/GO-pPy-KAN electrode response for the analytical tests. The detachment of the KAN molecules to obtain molecular imprints of KAN in pPy film was achieved by immersing GC/GO-pPy-KAN electrode in 0.01 M HCl solution (pH 2).

Besides, an electrode with pPy on the surface (GC/GO-pPy) was also developed using the same electropolymerization conditions without KAN to confirm the attachment of KAN molecules in the polymer matrix. Surface morphologies of GC/GO-pPy, GC/GO-pPy-KAN, and GC/GO-pPy-KAN* electrodes were investigated using AFM and XPS.

Fig. 3 shows AFM topography images taken using non-contact mode for an electrode area of 5 μm × 5 μm. Root mean square (RMS) values were also obtained from randomly chosen 5 different scan regions of the whole surface for 2 samples. A typical surface formation was observed for GC/GO electrode with a calculated RMS value of 71 ± 4 nm (Fig. 3 (a)) [40]. Moreover, typical polymer surface properties can also be seen from pPy modified GC/GO electrode with an RMS value of 44 ± 2 nm (Fig. 3(b)) [41]. Polymer coating reduced the surface roughness providing a more uniform electrode surface. The surface of the electrode remained similar to pPy modified electrode when KAN is used in the polymerization reaction with an RMS value of 34 ± 2 nm (Fig. 3(c)).

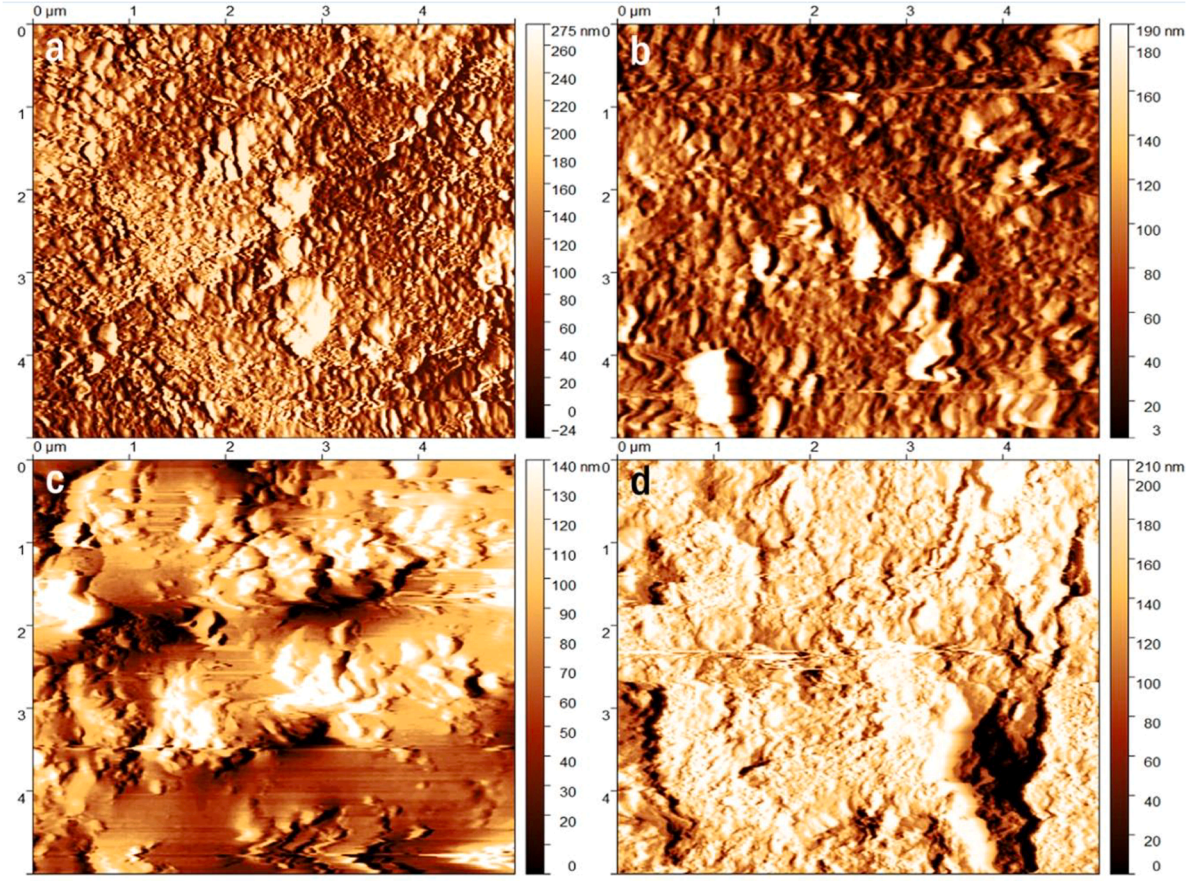

Fig. 3. AFM images of (a) GC/GO (b) GC/GO-pPy, (c) GC/GO-pPy-KAN, and (d) GC/GO-pPy-KAN* electrodes.

However, after the KAN molecules were detached from the polymer matrix, an RSM value of 52 ± 3 nm is obtained (Fig. 3(d)). This increase of the RSM value of GC/GO-pPY-KAN electrode shows that KAN molecules are successfully detached from the electrode, hence providing imprinted areas on the electrode surface.

The XPS spectra of GC/GO-pPy, GC/GO-pPy-KAN, and GC/GO-pPy-KAN* electrodes are shown in Fig. 4. As seen from Fig. 4(a) that N_{1s}, C_{1s} ve O_{1s} peaks are observed for GC/GO-pPy-KAN from survey XPS spectra which contains all the elements of the electrode preparation process. However, using C_{1s} ve O_{1s} peaks for the characterization wouldn't be suitable since all the prepared electrodes contain GO. Therefore, Fig. 4 (b) demonstrates a narrow region N_{1s} XPS core spectra of GC/GO-pPy, GC/GO-pPy-KAN, and GC/GO-pPy-KAN* electrodes. It can be seen that GC/GO-pPy electrode contains –NH functional group, however, GC/GO-pPy-KAN electrode contains both –NH and $–NH_2$ functional groups because KAN molecules have $–NH_2$ functional groups [42]. This indicates that the KAN molecules are successfully embedded in the polymer matrix. Moreover, a significant drop can be observed for the $–NH_2$ spectra when KAN molecules are detached from the polymer matrix confirming GC/GO-pPy-KAN* electrode is successfully obtained.

Fig. 5 shows the electrochemical characterization of the preparation steps for the electrodes using CV and EIS techniques performed in 1 mM $K_3Fe(CN)_6/K_4Fe(CN)_6$ redox probe at pH 7. It can be seen from the CV results (Fig. 5(a)) that GC/GO-pPy-KAN* electrode shows the highest peak current (14.37 ± 2.75 µA) among all other electrodes. However, this peak current value is very close to that obtained for GC/GO-pPy (13.56 ± 1.33 µA). This is due to the increase in the surface area of the electrode after imprinting KAN molecules. Although the polymer amount is the same, KAN molecules leave molecular imprints on the polymer surface increasing the total polymer surface area, thus more efficient electron transfer can be achieved between the electrode and the redox probe.

GC/GO electrode has a higher peak current value (8.92 ± 0.41 µA) from GC electrode (2.10 ± 0.12 µA) as expected because of the high electrical conductivity of GO. On the other hand, incorporation of the electroactive pPy further enhanced the electron transfer resulting in higher peak current densities than GC/GO electrode. This electrochemical behavior of the electrodes was further confirmed with EIS (Fig. 5(b)). The obtained Nyquist plots were fitted using equivalent circuit analysis and R_{ct} values were calculated (Table S1). The lowest R_{ct} value (0.2413 ± 0.0048) was obtained from GC/GO-pPy-KAN* confirming the CV results.

3.2. Optimization of parameters for MIP KAN sensor

To obtain the best performance for KAN detection from aqueous samples, preparation parameters of the electrodes were optimized using EIS performed in 1 mM $K_3Fe(CN)_6/K_4Fe(CN)_6$ redox probe at pH 7. Fig. 6 shows (a) the effect of different coating volumes of GO on GC electrode, (b) the effect of different KAN concentrations on electropolymerization of Py, (c) the time needed for HCl treatment and (d) the incubation time of 1 µM of KAN standard after modifying electrodes to obtain GC/GO-pPy-KAN* electrode confirmation (for each parameter, the rest of the parameters were kept constant as stated). This further modification to obtain GC/GO-pPy-KAN* is performed to see the real effect of the parameters on the performance of the final electrode confirmation.

First of all, GO volume coated on the GC electrode is optimized to avoid fouling that might occur due to excessive amounts of coatings and to control the film thickness for efficient electron transfer. The second optimization parameter for the electrode preparation is the amount of KAN used in the electropolymerization of Py since an excessive amount

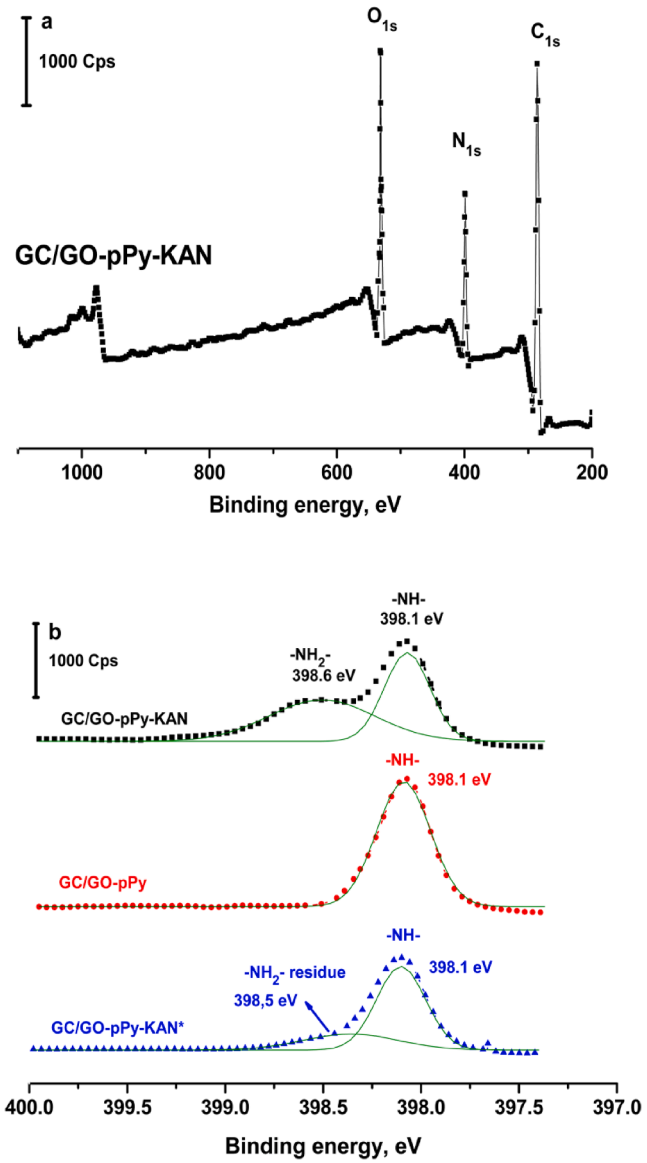

Fig. 4. (a) Survey XPS spectrum of GC/GO-pPy-KAN (b) N_{1s} XPS core spectra of GC/GO-pPy, GC/GO-pPy-KAN and GC/GO-pPy-KAN*.

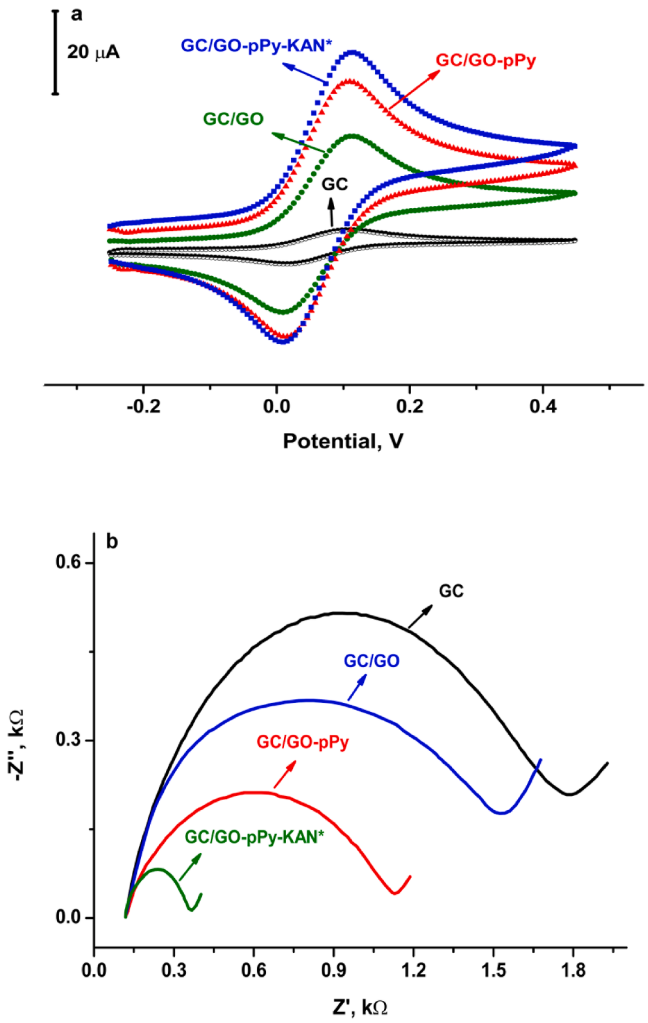

Fig. 5. (a) CVs (scan rate 200 mV/s) and (b) Nyquist plots (DC potential: 0.05 V, Frequency range between 300 kHz and 0.2 Hz) of GC (black), GO/GC (green), GC/GO-pPy (red) and GC/GO-pPy-KAN*(blue) in PBS solution (pH 7) containing 1 mM $K_3Fe(CN)_6/K_4Fe(CN)_6$ redox probe.

of KAN during polymerization might result in deformations on the polymer surface and affect the whole process. The optimum time required to completely remove the KAN molecules from GC/GO-pPy-KAN is another optimization parameter as remained KAN molecules might hinder results, hence, the sensitivity of the sensor.

Finally, incubation time, undoubtedly, is one of the most crucial parameters for MIP-based sensors since the time required for the target molecule to fully attach itself onto the imprinted polymer will determine how fast the determination process would take. The optimum parameters were mainly chosen based on the lowest R_{ct} values obtained from EIS, however, for incubation time, the highest R_{ct} value is used as optimum as it indicates the maximum attachment of the KAN molecules. Consequently, the optimum conditions were chosen as 10 μL of 20 mg/mL GO suspension for GO coating volume, 25 mM of KAN for polymerization reaction, 10 min HCl treatment time, and 30 min incubation time for the sensor development.

3.3. Analytical performance of the sensor

GC/GO-pPy-KAN* electrodes were prepared using optimized parameters to obtain the calibration curve and the analytical performance parameters of the sensor. The analytical detection range was chosen between 5 nM and 1 μM and predefined standard KAN solutions were applied on the sensor for 30 mins of incubation. Impedimetric analyses were performed after the incubation period in 1 mM $K_3Fe(CN)_6/K_4Fe(CN)_6$ redox probe at pH 7. Fig. 7 shows (a) the fitted Nyquist plots and (b) the calibration curve of the sensor. The R_{ct} values of the sensor increased with the increasing amounts of KAN used due to the strong binding of KAN molecules into the imprinted polymer matrix (Fig. 7(a)). These values then were plotted as a function of KAN concentration (Fig. 7(b)). It can be seen that the sensor showed a linear response ($R^2 = 0.99464$) for the given detection range with a LOD value of 5 nM. A complete list of analytical performance parameters was summarized in Table 1.

There have been different studies developed kanamycin sensors based on several detection strategies in the literature giving a wide range of LOD values (pM to nM) and sensitivities. However, the Korea Food and Drug Administration (KFDA) and the European Union reported that the MRL values for KAN in milk as 0.1 mg/kg (around 200 nM) and 0.15 mg/kg, respectively [43,44]. Therefore, although ultrasensitive detection of KAN can be possible, one must consider that simple, precise, accurate, and low-cost detection strategies providing a selective determination of KAN in milk samples are much more important considering the huge market for dairy products and the daily tests required

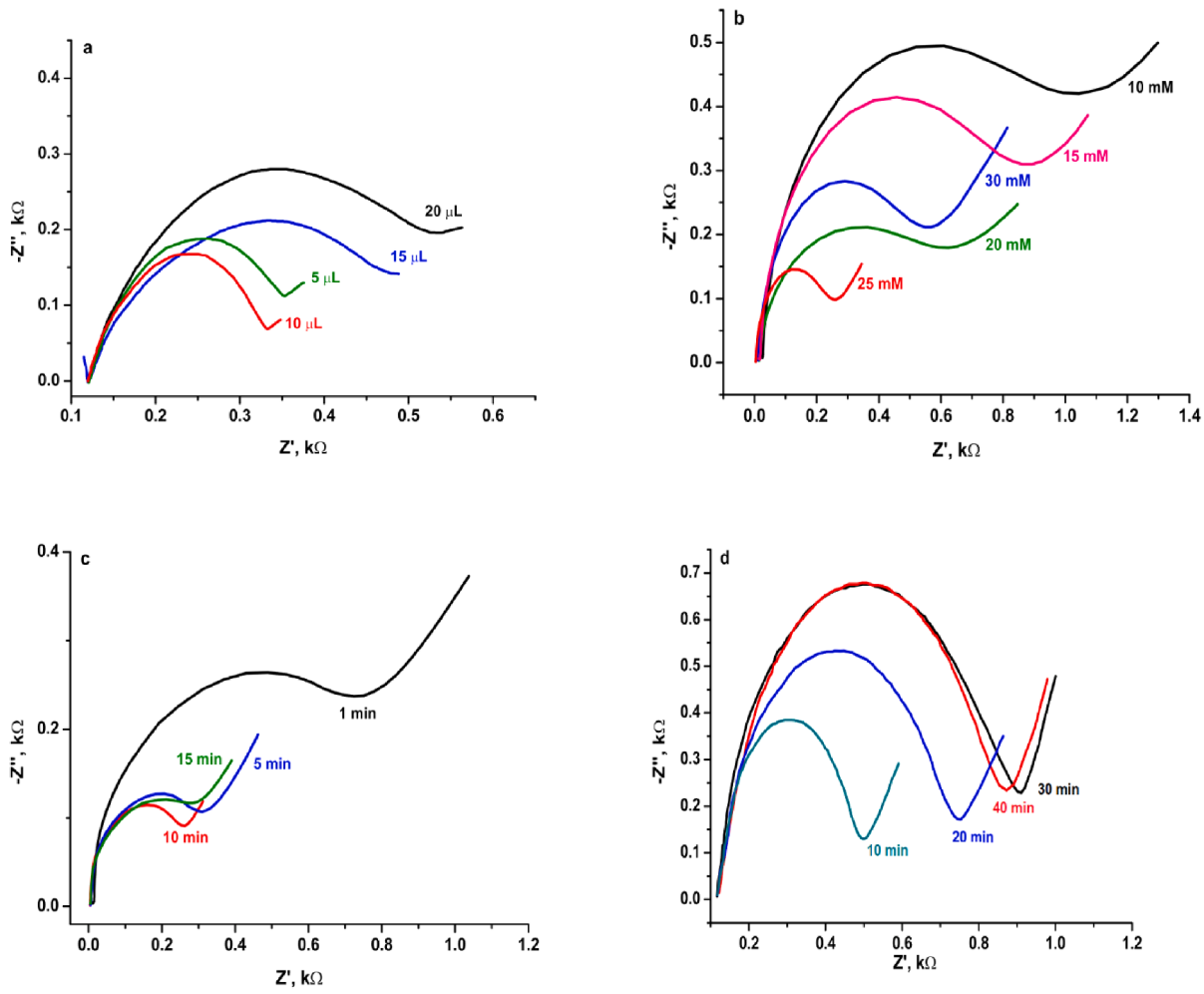

Fig. 6. Nyquist plots (DC potential: 0.05 V, Frequency range between 300 kHz and 0.2 Hz) showing (a) The effect of different coating volumes of GO on GC electrode, (b) the effect of different KAN concentrations on electropolymerization of Py, (c) the time needed for HCl treatment, and (d) the incubation time of 1 μM of KAN standard after modifying electrodes to obtain GC/GO-pPy-KAN* in PBS solution (pH 7) containing 1 mM $K_3Fe(CN)_6/K_4Fe(CN)_6$ redox probe.

worldwide. Considering the KFDA and EU regulations for KAN MRL ranges, the LOD value of this study is considered to be sufficient for the detection of KAN in milk samples.

Since the precise, accurate and selective determination of KAN is important for sensor development, precision and accuracy measurements were performed as intra-day and inter-day precision for 5 independent samples using 10 nM and 100 nM KAN (Table 2). Besides, inter-day precision measurements were also performed for 5 consecutive days. It can be seen from Table 2 that the developed sensor provides RSD % and relative error (RE) % values of $\leq$ 3.78% and $\leq$ 3.2%, respectively for both intra-day and inter-day measurements. Furthermore, Table 3 shows all the interfering substances and their % effects on R_{ct} values showing that $\leq$ 3.12% of R_{ct} change is obtained for the most interfering substance, TOB. Detailed precision, accuracy, and selectivity experiments showed that the prepared MIP-based KAN sensor showed reliable test results.

3.4. Determination of KAN in milk samples using developed MIP sensor

4 different commercial milk samples were used to test the performance of the developed MIP sensor for the determination of KAN. Table 4 shows the analytical determination and recovery values of KAN added to milk samples. It can be seen that recovery values between 92.7% and 104.3% were obtained with an average recovery value of 98.5%. This result shows that the determination of KAN from real samples such as milk is possible using the MIP-KAN sensor developed in this study within the MRL limits reported by KFDA and EU.

4. Conclusion

In this work, a novel MIP-KAN sensor was developed using pPy imprinted GO electrodes. CV and EIS results showed successful modification for each step of the electrode preparation process. Moreover, the detailed microscopic and spectroscopic analysis also confirmed the successful attachment and detachment of KAN molecules. All the preparation steps were also optimized to obtain reproducible and reliable results from the sensor. The calibration of the sensor was obtained using EIS between 5 nM and 1 μM with 5 nM LOD value. Furthermore, very good RSD% and RE% values for both intra-day and inter-day measurements were achieved. No significant interference was observed and very good recovery was obtained from commercial milk samples. Consequently, a novel, simple, and sensitive MIP-KAN sensor was developed using an easy and low-cost fabrication method for the detection of KAN in food samples such as milk.

CRediT authorship contribution statement

Deniz Işık: Investigation, Visualization. **Samet Şahin:** Writing - original draft, Supervision, Writing - review & editing. **Mustafa Oguzhan Caglayan:** Formal analysis, Data curation. **Zafer Üstündağ:**

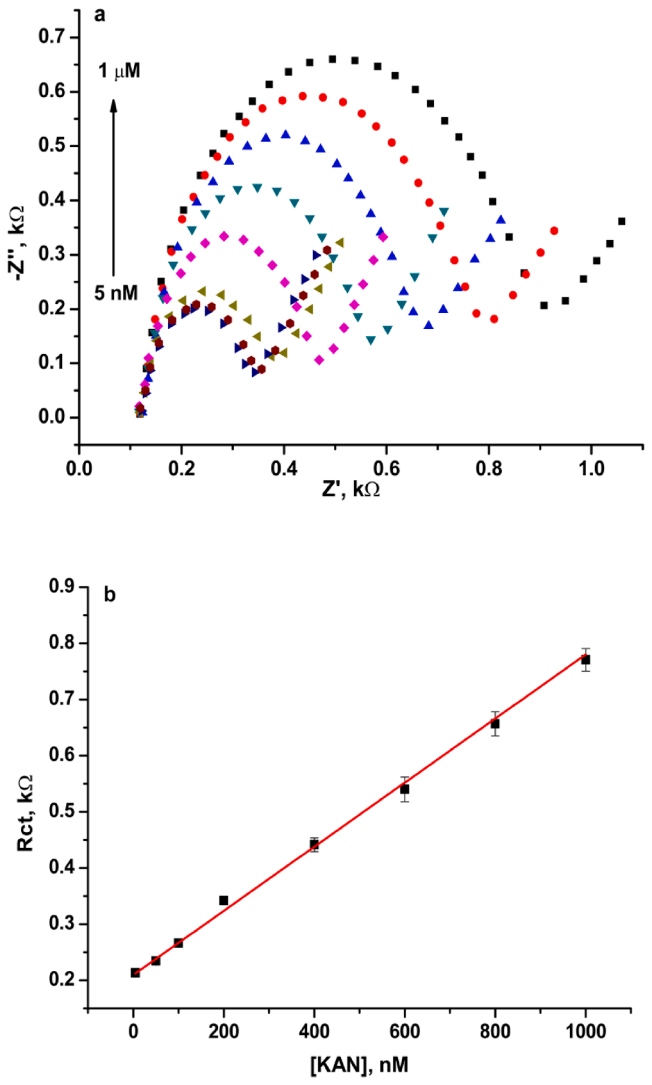

Fig. 7. (a) Nyquist curves (DC potential: 0.05 V, Frequency range between 300 kHz and 0.2 Hz) of GC/GO-pPy-KAN* electrodes incubated with different amounts of KAN samples. Tests were performed in PBS solution (pH 7) containing 1 mM $K_3Fe(CN)_6/K_4Fe(CN)_6$ redox probe. (b) Calibration curve of the sensor. Error bars are sample standard deviations (N = 5 samples).

Table 1
Analytical performance parameters of the sensor.

Analytical Parameter	Values
Linear Range	5 nM–1000 nM
Linear Equation (R_{ct}: kΩ; [KAN]: nM	R_{ct} = 0.21118 + 0.00057[KAN]
Standard error of slope,±	0.00002
Standard error of intercept,±	0.00270
R^2	0.9946
LOD†, nM	5
LOQ, nM	15

† LOD is defined as the lowest detectable analyte concentration. LOQ was calculated as 3 times of LOD value.

Conceptualization, Supervision, Resources, Writing - review & editing.

Declaration of Competing Interest

The authors declare that they have no known competing financial interests or personal relationships that could have appeared to influence the work reported in this paper.

Table 2
Precision and accuracy of the MIP-based KAN sensor. Error bars are sample standard deviations (N = 5 samples).

Added, nM	Intra-Day			Inter-Day		
	Found, nM	RSD %	RE %	Found, nM	RSD %	RE %
10	9.86 ± 0.18	1.83	−1.40	10.12 ± 0.13	1.28	+1.20
100	97.6 ± 3.6	3.69	−2.40	103.2 ± 3.9	3.78	+3.20

Table 3
The effect of possible interfering substances on MIP-based KAN sensor results (N = 5 samples).

Interference	Concentration (μM)	% R_{ct} Change
TOB	1	−3.12
GEN	1	−2.84
PEN	1	+1.91
AMX	1	−1.70

Table 4
Analytical determination and recovery of KAN added to milk samples.

Sample	Added, nM	Found, nM	% Recovery
Milk-1	0	0	–
	50	48.75	97.5
	100	104.28	104.3
	200	193.8	96.9
Milk-2	0	0	–
	50	46.35	92.7
	100	101.80	101.8
	200	193.9	97.0
Milk-3	0	–	–
	50	48.16	96.3
	100	101.13	101.1
	200	198.7	99.4
Milk-4	0	0	–
	50	47.65	95.3
	100	97.63	97.6
	200	203.5	101.7

Acknowledgments

This work includes a part of Ms. Deniz Işık's M.Sc. thesis. On behalf of all the authors, the corresponding authors state that there is no conflict of interest.

Appendix A. Supplementary data

Supplementary data to this article can be found online at https://doi.org/10.1016/j.microc.2020.105713.

References

[1] C. Wang, C. Liu, J. Luo, Y. Tian, N. Zhou, Direct electrochemical detection of kanamycin based on peroxidase-like activity of gold nanoparticles, Anal. Chim. Acta 936 (2016) 75–82.
[2] X. Zhang, J. Wang, Q. Wu, L. Li, Y. Wang, H. Yang, Determination of kanamycin by high performance liquid chromatography, Molecules 24 (10) (2019).
[3] Y.X. Zhou, W.J. Yang, L.Y. Zhang, Z.Y. Wang, Determination of kanamycin A in animal feeds by solid phase extraction and high performance liquid chromatography with pre-column derivatization and fluorescence detection, J. Liq. Chromatogr. Relat. Technol. 30 (11) (2007) 1603–1615.
[4] M.D. Yow, N.E. Tengg, J. Bangs, T. Bangs, W. Stephenson, The ototoxic effects of kanamycin sulfate in infants and children, J. Pediatr. 60 (1962) 230–242.
[5] L. Zhang, C. Zhu, C. Chen, S. Zhu, J. Zhou, M. Wang, P. Shang, Determination of kanamycin using a molecularly imprinted SPR sensor, Food Chem. 266 (2018) 170–174.

[6] H. Yang, Q. Wu, D. Su, Y. Wang, L. Li, X. Zhang, A label-free and turn-on fluorescence strategy for kanamycin detection based on the NMM/G-quadruplex Structure, Anal. Sci. 33 (2) (2017) 133–135.
[7] A. Zengin, U. Tamer, T. Caykara, Extremely sensitive sandwich assay of kanamycin using surface-enhanced Raman scattering of 2-mercaptobenzothiazole labeled gold@silver nanoparticles, Anal. Chim. Acta 817 (2014) 33–41.
[8] N.-R. Ha, I.-P. Jung, I.-J. La, H.-S. Jung, M.-Y. Yoon, Ultra-sensitive detection of kanamycin for food safety using a reduced graphene oxide-based fluorescent aptasensor, Sci. Rep. 7 (1) (2017) 1–10.
[9] B. Blanchaert, E.P. Jorge, P. Jankovics, E. Adams, A. Van Schepdael, Assay of kanamycin A by HPLC with direct UV detection, Chromatographia 76 (21–22) (2013) 1505–1512.
[10] N. Isoherranen, S. Soback, Chromatographic methods for analysis of aminoglycoside antibiotics, J.-AOAC Int. 82 (1999) 1017–1045.
[11] K.-M. Song, M. Cho, H. Jo, K. Min, S.H. Jeon, T. Kim, M.S. Han, J.K. Ku, C. Ban, Gold nanoparticle-based colorimetric detection of kanamycin using a DNA aptamer, Anal. Biochem. 415 (2) (2011) 175–181.
[12] Y. Tang, C. Gu, C. Wang, B. Song, X. Zhou, X. Lou, M. He, Evanescent wave aptasensor for continuous and online aminoglycoside antibiotics detection based on target binding facilitated fluorescence quenching, Biosens. Bioelectron. 102 (2018) 646–651.
[13] T. Kitagawa, K. Fujiwara, S. Tomonoh, K. Takashi, M. Koida, Enzyme immunoassays of kanamycin group antibiotics with high sensitivities using anti-kanamycin as a common antiserum: reasoning and selection of a heterologous enzyme label, J. Biochem. 94 (4) (1983) 1165–1172.
[14] Y. Zhu, P. Chandra, K.-M. Song, C. Ban, Y.-B. Shim, Label-free detection of kanamycin based on the aptamer-functionalized conducting polymer/gold nanocomposite, Biosens. Bioelectron. 36 (1) (2012) 29–34.
[15] F. Li, Y. Guo, X. Wang, X. Sun, Multiplexed aptasensor based on metal ions labels for simultaneous detection of multiple antibiotic residues in milk, Biosens. Bioelectron. 115 (2018) 7–13.
[16] M.F. Frasco, L.A. Truta, M.G.F. Sales, F.T. Moreira, Imprinting technology in electrochemical biomimetic sensors, Sensors 17 (3) (2017) 523.
[17] P.A. Cormack, A.Z. Elorza, Molecularly imprinted polymers: synthesis and characterisation, J. Chromatogr. B 804 (1) (2004) 173–182.
[18] T. Hishiya, H. Asanuma, M. Komiyama, Molecularly imprinted cyclodextrin polymers as stationary phases of high performance liquid chromatography, Polym. J. 35 (5) (2003) 440–445.
[19] G. Vlatakis, L.I. Andersson, R. Müller, K. Mosbach, Drug assay using antibody mimics made by molecular imprinting, Nature 361 (6413) (1993) 645–647.
[20] H. Yan, K.H. Row, Characteristic and synthetic approach of molecularly imprinted polymer, Int. J. Mol. Sci. 7 (5) (2006) 155–178.
[21] D. Zembrzuska, J. Kalecki, M. Cieplak, W. Lisowski, P. Borowicz, K. Noworyta, P. S. Sharma, Electrochemically initiated co-polymerization of monomers of different oxidation potentials for molecular imprinting of electroactive analyte, Sens. Actuators B 298 (2019), 126884.
[22] A. Adumitrăchioaie, M. Tertiș, A. Cernat, R. Săndulescu, C. Cristea, Electrochemical methods based on molecularly imprinted polymers for drug detection. A review, Int. J. Electrochem. Sci. 13 (2018) 2556–2576.
[23] Y. Teng, L. Fan, Y. Dai, M. Zhong, X. Lu, X. Kan, Electrochemical sensor for paracetamol recognition and detection based on catalytic and imprinted composite film, Biosens. Bioelectron. 71 (2015) 137–142.
[24] Z.Y. Guo, P.P. Gai, J. Duan, H.N. Zhang, S. Wang, Tetracycline selective electrode based on molecularly imprinted polymer particles, Chin. Chem. Lett. 21 (10) (2010) 1235–1238.
[25] V.K. Gupta, M.L. Yola, N. Özaltın, N. Atar, Z. Üstündağ, L. Uzun, Molecular imprinted polypyrrole modified glassy carbon electrode for the determination of tobramycin, Electrochim. Acta 112 (2013) 37–43.
[26] I. Kondratowicz, M. Nadolska, S. Şahin, M. Łapiński, M. Prześniak-Welenc, M. Sawczak, H.Y. Eileen, W. Sadowski, K. Żelechowska, Tailoring properties of reduced graphene oxide by oxygen plasma treatment, Appl. Surf. Sci. 440 (2018) 651–659.
[27] S. Yavuz, A. Erkal, İ.A. Kariper, A.O. Solak, S. Jeon, İ.E. Mülazımoğlu, Z. Üstündağ, Carbonaceous materials-12: a novel highly sensitive graphene oxide-based carbon electrode: preparation, characterization, and heavy metal analysis in food samples, Food Anal. Methods 9 (2) (2016) 322–331.
[28] İ.A. Kariper, M.O. Çağlayan, Z. Üstündağ, Heterogeneous Au/Ru hybrid nanoparticle decorated graphene oxide nanosheet catalyst for the catalytic reduction of nitroaromatics, Res. Chem. Intermed. 45 (2) (2019) 801–813.
[29] M. Yun, J.E. Choe, J.-M. You, M.S. Ahmed, K. Lee, Z. Üstündağ, S. Jeon, High catalytic activity of electrochemically reduced graphene composite toward electrochemical sensing of Orange II, Food Chem. 169 (2015) 114–119.
[30] İ. Üstündağ, A. Erkal, T. Koralay, Y.K. Kadıoğlu, S. Jeon, Gold nanoparticle included graphene oxide modified electrode: Picomole detection of metal ions in seawater by stripping voltammetry, J. Anal. Chem. 71 (7) (2016) 685–695.
[31] S. Hou, S. Su, M.L. Kasner, P. Shah, K. Patel, C.J. Madarang, Formation of highly stable dispersions of silane-functionalized reduced graphene oxide, Chem. Phys. Lett. 501 (1–3) (2010) 68–74.
[32] A. Erkal, İ. Üstündağ, S. Yavuz, Z. Üstündağ, An Electrochemical application of MnO2 decorated graphene supported glassy carbon ultrasensitive electrode: Pb2+ and Cd2+ analysis of seawater samples, J. Electrochem. Soc. 162 (4) (2015) H213.
[33] Z. Üstündağ, A.O. Solak, EDTA modified glassy carbon electrode: preparation and characterization, Electrochim. Acta 54 (26) (2009) 6426–6432.
[34] H. De Ruyck, H. De Ridder, Determination of tetracycline antibiotics in cow's milk by liquid chromatography/tandem mass spectrometry, Rapid Commun. Mass Spectrom. 21 (9) (2007) 1511–1520.
[35] Y. Kong, W. Zhao, S. Yao, J. Xu, W. Wang, Z. Chen, Molecularly imprinted polypyrrole prepared by electrodeposition for the selective recognition of tryptophan enantiomers, J. Appl. Polym. Sci. 115 (4) (2010) 1952–1957.
[36] A. Ramanaviciene, A. Ramanavicius, Molecularly imprinted polypyrrole-based synthetic receptor for direct detection of bovine leukemia virus glycoproteins, Biosens. Bioelectron. 20 (6) (2004) 1076–1082.
[37] I. Sadriu, S. Bouden, J. Nicolle, F.I. Podvorica, V. Bertagna, C. Berho, L. Amalric, C. Vautrin-Ul, Molecularly imprinted polymer modified glassy carbon electrodes for the electrochemical analysis of isoproturon in water, Talanta 207 (2020), 120222.
[38] Z.O. Uygun, Y. Dilgin, A novel impedimetric sensor based on molecularly imprinted polypyrrole modified pencil graphite electrode for trace level determination of chlorpyrifos, Sens. Actuators B 188 (2013) 78–84.
[39] M.M. Gvozdenović, B. Jugović, J.S. Stevanović, B. Grgur, Electrochemical synthesis of electroconducting polymers, Hemijska industrija 68 (6) (2014) 673–684.
[40] A.S. Adekunle, B.O. Agboola, J. Pillay, K.I. Ozoemena, Electrocatalytic detection of dopamine at single-walled carbon nanotubes–iron (III) oxide nanoparticles platform, Sens. Actuators B 148 (1) (2010) 93–102.
[41] K.C. Persaud, Polymers for chemical sensing, Mater. Today 8 (4) (2005) 38–44.
[42] H. He, Y. Hu, S. Chen, L. Zhuang, B. Ma, Q. Wu, Preparation and properties of a hyperbranch-structured polyamine adsorbent for carbon dioxide capture, Sci. Rep. 7 (1) (2017) 1–10.
[43] Y. Wang, M. Zou, Y. Han, F. Zhang, J. Li, X. Zhu, Analysis of the kanamycin in raw milk using the suspension array, J. Chem. 2013 (2012).
[44] C.-M. Lim, B.-H. Cho, G.-S. Chung, S.-W. Son, Determination of aminoglycosides in milk by liquid chromatography with tandem mass spectrometry, Kor. J. Vet. Publ. Hlth 36 (2012) 121–130.